



Abstract

20

21 Surface incident solar radiation ( $R_s$ ) plays a key role in climate change on Earth.  $R_s$  can  
22 be directly measured, and it shows substantial variability on decadal scales, i.e., global  
23 dimming and brightening.  $R_s$  can also be derived from the observed sunshine duration  
24 (SunDu) with reliable accuracy. The SunDu-derived  $R_s$  has been used as a reference to  
25 detect and adjust the inhomogeneity in the observed  $R_s$ . However, both the observed  $R_s$   
26 and SunDu-derived  $R_s$  may have inhomogeneity. In Japan, SunDu has been measured  
27 since 1890, and  $R_s$  has been measured since 1961 at ~100 stations. In this study, the  
28 observed  $R_s$  and SunDu-derived  $R_s$  were first checked for inhomogeneity independently  
29 using a statistical software RHtest. If confirmed by the metadata of these observations,  
30 the detected inhomogeneity was adjusted based on the RHtest-quantile matching  
31 method. Second, the two homogenized time series were compared to detect further  
32 possible inhomogeneity. If confirmed by the independent ground-based manual  
33 observations of cloud cover fraction, the detected inhomogeneity was adjusted based  
34 on the reference dataset. As a result, a sharp decrease of more than  $20 \text{ W m}^{-2}$  in the  
35 observed  $R_s$  from 1961 to 1975 caused by instrument displacement was detected and  
36 adjusted. Similarly, a decline of about  $20 \text{ W m}^{-2}$  in SunDu-derived  $R_s$  due to steady  
37 instrument replacement from 1985 to 1990 was detected and adjusted too. After  
38 homogenizations, the two estimates of  $R_s$  agree well. The homogenized SunDu-derived  
39  $R_s$  show an increased at a rate of  $0.9 \text{ W m}^{-2}$  per decade ( $p < 0.01$ ) from 1961 to 2014,  
40 which was caused by a positive aerosol-related radiative effect ( $2.2 \text{ W m}^{-2}$  per decade)

41 and a negative cloud cover radiative effect ( $-1.4 \text{ W m}^{-2}$  per decade). The brightening  
42 over Japan was the strongest in spring, likely due to a significant decline in aerosol  
43 transported from Asian dust storms. The observed raw  $R_s$  data and their homogenized  
44 time series used in this study are available at  
45 <https://doi.org/10.11888/Meteoro.tpsc.271524> (Ma et al., 2021).

## 46 **1. Introduction**

47 Surface incident solar radiation ( $R_s$ ) plays a vital role in atmospheric circulation,  
48 hydrologic cycling and ecological equilibrium; therefore, its decrease and increase  
49 termed as global dimming and brightening (Wild et al., 2005; Shi et al., 2008), have  
50 received widespread interest from the public and scientific community (Allen et al.,  
51 2013; Xia, 2010; Wang et al., 2013; Tanaka et al., 2016; Ohmura, 2009; He et al., 2018).

52 In addition, the impact factors such as clouds and aerosols on the variation in  $R_s$  have  
53 been widely studied (Wild et al., 2021; Qian et al., 2006; Feng and Wang, 2021a).

54 Ground-based observations of  $R_s$  are the first recommendation for detecting global  
55 dimming and brightening. However, observational data may be inevitably ruined by  
56 artificial shifts, which may lead to the variability in  $R_s$  with large uncertainties. Wang et  
57 al. (2015) point out that instrument replacements and reconstruction of observational  
58 network introduced substantial inhomogeneity into the time series of observed  $R_s$  over  
59 China for 1990-1993. Manara et al. (2016) also show the instrument changes from the  
60 Robitzsch pyranograph to the Kipp & Zonen CM11 pyranometer before 1980 caused  
61 no clear dimming in Italy. Until recently, Wild et al. (2021) use a well-maintained data  
62 series at a site in Germany with long time duration to investigate the dimming and  
63 brightening in central Europe under clear sky condition, and point out that the aerosol  
64 pollutants are likely major drivers in the  $R_s$  variations. Augustine and Hodges (2021)  
65 use Surface Radiation Budget (SURFRAD) Network observations to explore the

66 variability in  $R_s$  over the U.S. from 1996 to 2019, and find that cloud fraction can  
67 explain 62% of the variation of  $R_s$ , while aerosol optical depth (AOD) only accounts  
68 for 3%. Both studies also indicate the measurement instruments have been changed  
69 over the observational time periods, which may introduce non-climatic shifts and  
70 inhomogeneity in the raw data series.

71 Homogenizing the observed  $R_s$  has been attempted in China (Wang et al., 2015;  
72 Tang et al., 2011; Yang et al., 2018), Italy (Manara et al., 2016), Spain (Sanchez-  
73 Lorenzo et al., 2013) and Europe (Sanchez-Lorenzo et al., 2015). It is essential to find  
74 a homogeneous reference station to compare with the possible inhomogeneous station  
75 to test and adjust the inhomogeneity in the observed time series, as done for the  
76 homogenization of air temperature (Du et al., 2020; Zhou et al., 2021). However, this  
77 process is difficult for  $R_s$  because the instrument replacement of  $R_s$  generally occurs  
78 nearly simultaneously throughout a country. Therefore, the sunshine duration (SunDu)  
79 derived  $R_s$  (Yang et al., 2006) has been used as a homogeneous reference dataset to  
80 detect and adjust the inhomogeneity of  $R_s$  in China (Wang et al., 2015).

81 The SunDu records the hours of surface direct solar radiation exceeding  $120 \text{ W m}^{-2}$   
82 and provides an alternative way to estimate  $R_s$  (Yang et al., 2006; Stanhill and Cohen,  
83 2008). SunDu-derived  $R_s$  is capable of capturing the variability in  $R_s$ . He et al. (2018)  
84 use the SunDu-derived  $R_s$  at  $\sim 2600$  stations to revisit the global dimming and  
85 brightening over different continents, and restate the dimming over China and Europe  
86 is consistent with the increasing trends of clouds and aerosols. Feng and Wang (2021b)

87 and Feng and Wang (2021a) merge the satellite retrievals with SunDu-derived  $R_s$  to  
88 produce a high-resolution long-term solar radiation over China, and indicate cloud  
89 fraction could explain approximately 86%–97% of  $R_s$  variation. Zeng et al. (2020)  
90 demonstrate that SunDu plays a dominant role in determining  $R_s$  based on a random  
91 forest model framework across China. Stanhill and Cohen (2005) indicate the high  
92 correlation between SunDu and  $R_s$  at the 26 stations in the United States. Sanchez-  
93 Lorenzo et al. (2008) show the variation in SunDu is consistent with that in  $R_s$  over  
94 western Europe for 1938-2004, and the SunDu time evolution in Spring can partly be  
95 explained by clouds and that in Winter can be related to the anthropogenic aerosol  
96 emissions. Stanhill and Cohen (2008) establish a simple linear relationship between  $R_s$   
97 and SunDu to determine the long-term variation in  $R_s$  over Japan. Manara et al. (2017)  
98 highlight that the atmospheric turbidity should be considered when using SunDu for  
99 investigating multidecadal evolution of  $R_s$ .

100 Artificial shifts in SunDu observations may come from the replacement of  
101 instruments. It has been revealed that the Jordan recorder is 10% more sensitive than  
102 the Campbell-Stokes recorder for SunDu measurements (Noguchi, 1981). The  
103 homogenization of SunDu has been carried out in Iberian Peninsula (Sanchez-Lorenzo  
104 et al., 2007), Switzerland (Sanchez-Lorenzo and Wild, 2012), and Italy (Manara et al.,  
105 2015).

106 The measurement of  $R_s$ , which started in 1961 in Japan, has a long history (Tanaka  
107 et al., 2016), and a data record more than half a century-long has been accumulated.

108 The dataset has been widely used to study decadal variability (Wild et al., 2005; Stanhill  
109 and Cohen, 2008) and to evaluate model simulations (Allen et al., 2013; Dwyer et al.,  
110 2010). The Eppley and Robitzsch pyranometers used to measure  $R_s$  over Japan were  
111 replaced by the Moll-Gorczyński thermopile pyranometers in the early 1970s (Tanaka  
112 et al., 2016). However, the possible inhomogeneity of the observed  $R_s$  over Japan has  
113 not been well quantified, and most existing studies directly used raw  $R_s$  data (Wild et  
114 al., 2005; Tanaka et al., 2016; Tsutsumi and Murakami, 2012; Allen et al., 2013; Wild  
115 and Schmucki, 2011; Kudo et al., 2012; Ohmura, 2009). Some studies have had to  
116 abandon data from the early years and focused on only  $R_s$  data collected after 1975  
117 (Tsutsumi and Murakami, 2012; Dwyer et al., 2010). Therefore, the observed decadal  
118 variability in  $R_s$  over Japan is questionable, especially for the 1961-1975 time period.

119 In Japan, SunDu observations started in 1890, and more than a century-long data  
120 were recorded. They cannot be too precious for the climate change detection on a  
121 century scale. It is reported that the Jordan recorders used to measure SunDu were  
122 replaced by EKO rotating mirror recorders in approximately 1986 (Inoue and  
123 Matsumoto, 2003; Stanhill and Cohen, 2008). Therefore, SunDu observations over  
124 Japan themselves may suffer inhomogeneity issues.

125 Non-climatic shifts in the observations may severely influence the climate  
126 assessment, therefore rigorous homogenization are required. The world Meteorological  
127 Organization (WMO) Climate Program guidelines on climate metadata and  
128 homogenization list 14 data homogenization assessment techniques developed and

129 applied by different groups/authors (Aguilar et al., 2003). Reeves et al. (2007)  
130 compared eight representative homogenization methods and provided guidelines for  
131 which procedures work best in different situation, for example the standard normal  
132 homogeneity (SNH) test (Alexandersson, 1986) works best if good reference series are  
133 available and two-phase regressions of Wang procedure (Wang, 2003) is optimal for  
134 good reference series unavailable condition. Based on the comparison work, RHtest  
135 method was improved by detecting multiple changepoints in the climate data no matter  
136 the reference series are available (Wang, 2008b; Wang et al., 2010; Wang et al., 2007;  
137 Wang, 2008a). This method, which first detects the changepoints in a series using  
138 penalized maximal tests and then tunes the inhomogeneous data segments to be  
139 consistent with other segments in empirical distributions, has been widely used in  
140 homogenizing climate variables (Dai et al., 2011; Wang et al., 2010; Du et al., 2020;  
141 Zhou et al., 2021).

142 Discontinuities are inevitably occurred in the long-term observation system which  
143 are required to be checked out and adjusted in the raw data. The homogenized series  
144 pose a significant role in realistic and reliable assessment of climate trend and  
145 variability. The main objective of this study is to detect and adjust the inhomogeneity  
146 in  $R_s$  estimates over Japan. The metadata were first extracted from website information  
147 and related records at each site. The SunDu observations were converted into  $R_s$ . The  
148 RHtest method was applied to homogenize the observed  $R_s$  and SunDu-derived  $R_s$ , and  
149 finally, the century-long homogenized  $R_s$  data were produced over Japan. Furthermore,



150 the impacts of cloud cover and aerosols on  $R_s$  variation over Japan in recent decades  
151 were explored.

## 152 **2. Data and methods**

### 153 **2.1 Surface incident solar radiation and sunshine duration**

154 The monthly observed  $R_s$  at 105 stations and SunDu at 156 stations were  
155 downloaded from the Japanese Meteorology Agency (JMA) website (see Table S1 and  
156 Figure 1).  $R_s$  records were available from 1961. During the 1960s, two  $R_s$  measurements  
157 were conducted in parallel by both Eppley and Robitzsch pyranometers. In the early  
158 1970s (see Figure 2 and Table S2), these instruments were replaced by Moll-Gorczynski  
159 thermopile pyranometers. This replacement occurred at approximately 12.4% of  $R_s$   
160 stations in 1971, followed by 22.9%, 24.8%, 3.8% and 30.5% in the next four years,  
161 which may have caused severe data discontinuity problems (Tanaka et al., 2016).

162 SunDu has been routinely measured since 1890. Jordan recorders were replaced  
163 by EKO rotating mirror recorders at 49.4% of SunDu stations in 1986. Until 1990,  
164 nearly all of the SunDu stations used new instruments for observations. 4.5% of SunDu  
165 stations before 1985 and 9.0% of SunDu stations after 2000 were moved away from the  
166 original sites (see Figure 2 and Table S2) (Stanhill and Cohen, 2008).

167 In this study, SunDu was used to derive  $R_s$  based on the following equation (Yang  
168 et al., 2006):

$$169 \quad R_s / R_c = a_0 + a_1 \cdot n / N + a_2 \cdot (n / N)^2 \quad (1)$$

170 where  $n$  is sunshine duration hours;  $N$  is the maximum possible sunshine duration;  $R_c$   
171 is surface solar radiation under clear skies; and  $a_0$ ,  $a_1$  and  $a_2$  are coefficients. This  
172 method was recommended in many studies (Wang et al., 2015; Tang et al., 2011).

## 173 2.2. Homogenization method

174 Both  $R_s$  and SunDu measurements over Japan suffer severe inhomogeneity  
175 problems, which require rigorous data homogenization. RHtest  
176 (<http://etccdi.pacificclimate.org/software.shtml>) is a widely used method to detect and  
177 adjust multiple changepoints in a climate data series, such as in surface temperature  
178 (Du et al., 2020), radiosonde temperature (Zhou et al., 2021), precipitation (Wang et al.,  
179 2010) and surface incident solar radiation (Yang et al., 2018). [RHtest provides two](#)  
180 [algorithms, the ~~were provided to detect changepoints based on the~~](#) penalized maximal  
181 T (PMT) test (Wang et al., 2007) and the penalized maximal F (PMF) test (Wang,  
182 [2008b\), to detect changepoints](#). The problem of lag-1 autocorrelation in detecting mean  
183 shifts in time series was also resolved (Wang, 2008a). The PMT algorithm requires the  
184 base time series to be no trend, and hence a reference series is needed. It is invalid when  
185 a reference series is not often available or its homogeneity is not sure, also the trend in  
186 the base and reference series are probably different. The PMF algorithm allows the time  
187 series in a constants trend and thus is applicable without a reference series. Both  
188 algorithms have higher detection power and the false alarm rate can be reduced by  
189 empirically constructed penalty function.

190 As the change of instrument in  $R_s$  and SunDu observation nearly happened

191 nationwide and simultaneously, it is difficult to find reference data series to match the  
192 base data series and hence the PMF algorithm was used to detect the changepoints in  
193 this study. Multiple changepoints were detected including climate signals and artificial  
194 shifts, and only the ones confirmed by discontinuity information from metadata in Table  
195 S2 were left to be adjusted. Then two homogenized series based on direct measurement  
196 of  $R_s$  and SunDu-derived  $R_s$  were obtained.

197 Large uncertainties may still exist in both homogenized data series as the  
198 discontinuities in the raw observations may not be sufficiently and correctly recorded  
199 in the metadata. Further changepoints can be detected by considering the impact of the  
200 variation of independent climate variables such as clouds and aerosols on the  $R_s$   
201 variation. If these uncertainties were found, further changepoint detections were needed  
202 based on the PMT or PMF algorithm.

203 To diminish all significant artificial shifts caused by the changepoints, a newly  
204 developed Quantile-Matching (QM) adjustments in the RHtest (Vincent et al., 2012;  
205 Wang et al., 2010) were performed to adjust the series so that the empirical distributions  
206 of all segments of the detrended base series agree with each other. The corrected values  
207 are all based on the empirical frequency of the datum to be adjusted.

208 Another independent homogenization method proposed by Katsuyama (1987),  
209 which was developed due to the replacement of the Jordan recorders with EKO rotating  
210 mirror recorder during the late 1980s, is denoted as follows:

$$211 \quad S_R = 0.8 S_J (S_J < 2.5 \text{ h/day}) \quad (2)$$

212 
$$S_R = S_J - 0.5 \text{ h/day} (S_J \geq 2.5 \text{ h/day}) \quad (3)$$

213 where  $S_J$  is the daily SunDu observed by the Jordan recorders before replacement; and  
214  $S_R$  is the daily SunDu adjusted to be consistent with the values observed with the EKO  
215 rotating mirror recorders.

216 These two homogenization methods were compared in this study and yielded  
217 nearly the same SunDu-derived  $R_s$  variation, as shown in Figure 3. Although the  
218 second method proposed by Katsuyama (1987) is simple and efficient, we just use it  
219 to cross validate the accuracy of the RHtest method. ~~For the following analysis, the~~  
220 ~~SunDu-derived  $R_s$  homogenized by RHtest was used as RHtest method provides~~  
221 ~~higher power to detect the changepoints in a data series no matter the metadata are~~  
222 ~~available.~~ Since most artificial shifts in observation system were undocumented  
223 worldwide, the statistical methods including RHtest are optimal to identify these non-  
224 climatic signals and reduce the discontinuities in the data series. As RHtest can detect  
225 the changepoints in the raw data series when the metadata are unavailable while  
226 Katsuyama (1987) can't, and RHtest was therefore selected in this study.

### 227 **2.3 Clouds**

228 Clouds play an important role in  $R_s$  variation (Norris and Wild, 2009). Monthly  
229 cloud cover observations at 155 stations were also available on the JMA website. The  
230 observation time for cloud amount has been 08:00-19:00 since 1981 at 9.0% of cloud  
231 amount stations and 08:30-17:00 from 1990 to 1995 at another 15.4% of cloud amount  
232 stations (see Figure 2 and Table S2). However, the difference between annual raw and

233 homogenized cloud data is trivial, as cloud data are relatively homogeneous in space  
234 compared with  $R_s$  and SunDu observations. A site observation of cloud amount can  
235 represent the value over a large spatial scale, likely leading to few inhomogeneity issues  
236 for cloud data.

237 To explore the impact of the cloud cover anomaly on the  $R_s$  variation, the cloud  
238 cover radiative effect (CCRE), defined as the change in  $R_s$  produced by a change in  
239 cloud cover, was proposed by (Norris and Wild, 2009):

$$240 \quad CCRE' (lat, lon, y, m) = CC' (lat, lon, y, m) \times CRE(g, m) / \overline{CC}(g, m) \quad (4)$$

241 where  $lat$  is the latitude,  $lon$  is the longitude,  $y$  is the year,  $m$  is the month,  $CCRE'$   
242 is the cloud cover radiative effect anomaly,  $CC'$  is the cloud cover anomaly,  $\overline{CC}$  is  
243 the climatology of cloud cover in 12 months and  $CRE$  is the cloud radiative effect  
244 calculated by the  $R_s$  difference under all sky and clear sky conditions.

245 The residual radiative effect was determined by removing the CCRE anomalies  
246 from the  $R_s$  anomalies. It is noted that a part of the cloud albedo radiative effect  
247 proportional to the cloud amount was contained in the CCRE, as a large cloud amount  
248 tends to yield enhanced cloud albedo, whereas another part of the cloud albedo radiative  
249 effect due to the aerosol first indirect effect (more aerosols facilitating more cloud  
250 condensation nuclei may enhance cloud albedo) may be included in the residual  
251 radiative effect, which mainly contains the aerosol radiative effect.

252 The Clouds and the Earth's Radiant Energy System (CERES) provides a reliable  
253 surface incident solar radiation (Ma et al., 2015) primarily based on the Moderate

254 Resolution Imaging Spectroradiometer (MODIS) cloud and aerosol products (Kato et  
255 al., 2012). The cloud amount in CERES agrees well with the observations, and the  
256 annual CRE in CERES is well correlated with the annual cloud amount in Figure 10.  
257 The regional average cloud amount over Japan in Figure 10 (blue line) increases at a  
258 rate of 0.7% per decade from 1960 to 2015, which is consistent with the previous results  
259 (Figure 4 in Tsutsumi and Murakami (2012)).

260 In this study, long-term observations of cloud amount and monthly cloud radiative  
261 effect (CRE) data in the CERES EBAF edition were used following Equation (4) to  
262 distinguish the cloud cover radiative effect from  $R_s$  variation.

## 263 **2.4 Data Processing**

264 We first interpolated the monthly observational data at sites into  $1^\circ \times 1^\circ$  grid data,  
265 and then calculated the area average of the climate variables. As the brightening and  
266 dimming over Japan were the main concern in this study, monthly values were  
267 converted into annual values for calculation. If there are missing values in any month  
268 in a specific year, the annual value for that year is set to a missing value. The linear  
269 regression was used for trend calculation.

## 270 **3. Results**

271 In this section, we first compared the observed  $R_s$  and sunshine duration derived  
272  $R_s$  before and after adjustment to demonstrate the necessity and feasibility of the  
273 homogenization procedure in Section 3.1. As artificial shifts may not be sufficiently

274 and correctly documented by metadata, uncertainties may still exist in the homogenized  
275 series. We then tried to explore these uncertainties by considering the influence of other  
276 independent climate variables such as clouds, aerosols on the  $R_s$  variation, and  
277 ultimately informed a more reasonable homogenized  $R_s$  series in Section 3.2. In Section  
278 3.3, we claimed the significant correction in trend analysis of  $R_s$  in Japan and quantified  
279 the influence of clouds and aerosols on the  $R_s$  variation.

### 280 **3.1 Homogenization of observed $R_s$ and sunshine duration derived $R_s$**

281 The comparisons between raw data and homogenized data at each site were  
282 shown in Figure 4 and their difference were illustrated in Figure 5. Compared with  
283 raw data, the absolute values of biases between  $R_s$  and SunDu-derived  $R_s$  at 74 stations  
284 decrease after homogenization, of which the absolute values of biases decrease by  
285 more than  $4 \text{ W m}^{-2}$  at 42 stations and more than  $10 \text{ W m}^{-2}$  at 8 stations. The root mean  
286 square errors at 80 stations were reduced after homogenization, of which reduces are  
287 more than  $4 \text{ W m}^{-2}$  at 40 stations. After adjustments, the correlation coefficients  
288 between the annual observed  $R_s$  and annual SunDu-derived  $R_s$  are improved at 68  
289 stations, including greater than 0.2 improvement at 31 stations. There are 41 stations  
290 (marked with red in Table S1, Figure 6) at which the correlation coefficients were  
291 greater than 0.5, and the biases and the root mean square errors generally decrease  
292 after homogenization.

293 Figure 7, as an example, shows the time series of surface incident solar radiation  
294 ( $R_s$  and SunDu-derived  $R_s$ ) at the HAMADA site (WMO-ID: 47755, Lat: 34.9, Lon:

295 132.07) before and after homogenization. Details in the improvements after  
296 homogenization at most stations can be traced back to Figures 4, 5 and 6. The  
297 improved patterns of time series of surface incident solar radiation after  
298 homogenization highlights the necessity and feasibility of the RHtest method. The  
299 SunDu-derived  $R_s$  variation over Japan during recent decades inferred from these  
300 “perfect” data at 41 sites (Figure 8) was nearly identical to that from all available data  
301 at 156 sites (as shown in Table 1 and Figure 9).

### 302 **3.2 Uncertainties in $R_s$ observations**

303 Figure 9 displays the change in  $R_s$  during the last 5 decades, while Figure 10 shows  
304 the variation in observed clouds over Japan. The sharp decrease in  $R_s$  in 1963 caused  
305 by the volcanic eruption of Agung in Indonesia (Witham, 2005) can be clearly found.  
306 The sharp decreases in  $R_s$  in 1991 and 1993 are due to the combined effect of the  
307 volcanic eruption of Mount Pinatubo in the Philippines in 1991 (Robock, 2000) and the  
308 simultaneous significant increases in clouds (Figure 8 in Tsutsumi and Murakami  
309 (2012)). The volcanic eruption of El Chichón in Mexico in 1982 exerted little impact  
310 on the decline in  $R_s$  and may have been compensated by the decrease in clouds, as shown  
311 in Figure 10. The pronounced  $R_s$  decline in 1980 coincides with the significant increase  
312 in clouds, while the lightening of  $R_s$  in 1978 and 1994 encounters abrupt decreases in  
313 cloud covers.

314 As shown in Figure 9, no major modifications were found in  $R_s$  observations  
315 before and after homogenization (comparison between the light blue and dark blue



316 lines). However, the SunDu-derived  $R_s$  series are smoother after adjustment by the QM  
317 method, as the sharp decrease from 1983 to 1993 caused by the replacement of sunshine  
318 duration instruments (Jordan recorders were replaced with EKO rotating mirror  
319 recorders) (Stanhill and Cohen, 2008) was repaired (comparison between the light red  
320 line and dark red lines). Despite the identical increase in  $R_s$  via both the homogenized  
321 direct measurements of  $R_s$  and the homogenized SunDu-derived  $R_s$  during the 1995-  
322 2014 period, their variations in  $R_s$  from 1961 to 1994 are different (dark red line and  
323 dark blue line).

324 Large discrepancies in  $R_s$  variation were found during the time period of 1961-  
325 1970, although homogenizations were performed on the direct measurements of  $R_s$  and  
326 SunDu-derived  $R_s$  (dark blue line and dark red line in Figure 9). Existing study noted  
327 the inaccurate instruments used at the beginning of operation in the  $R_s$  observation  
328 network in approximately 1961, and the parallel use of two different types of  
329 instruments during the 1960s may result in the large variability in observed  $R_s$  (Tanaka  
330 et al., 2016). At this time, the clouds fluctuated gently, as shown in Figure 10, and the  
331 change in volcanic aerosols from 1965 to 1966 was nearly the same as that from 1962  
332 to 1963 (Table 2 in Sato et al. (1993)), so the sudden decline in the direct observations  
333 of  $R_s$  from 1965 to 1966, which was twice as large as that from 1962 to 1963, is  
334 suspicious. It is inferred that anthropogenic aerosols play a subtle role in the significant  
335 reduction in  $R_s$ , as this type of phenomenon is common for both polluted and pristine  
336 stations in Japan (Figure 22 in (Tanaka et al., 2016)).

337 Figure 11 shows the correlation coefficients between homogenized  $R_s$  (observed  
338 and SunDu-derived) and cloud amount. In general, the observed  $R_s$  (-0.45) is less  
339 correlated than the SunDu-derived  $R_s$  (-0.67), particularly from 1961 to 1970, -0.21  
340 compared with -0.64. This in turn supports the reliability of homogenized SunDu-  
341 derived  $R_s$ , especially during the time period of 1961-1970. The false variability of the  
342 observed  $R_s$  from 1961 to 1970 was modified by the RHtest method against the  
343 homogenized SunDu-derived  $R_s$  as shown in Figure 12.

344 General decreases in stratospheric aerosol optical depth (AOD) were reported in  
345 Sato et al. (1993) from 1965 to 1980, and clouds fluctuated slightly, as shown in Figure  
346 10; both of these factors contributed to a brightening of  $R_s$ . This is in agreement with  
347 the SunDu-derived  $R_s$  and contrasts with the direct measurements of  $R_s$ .

348 During the 1985-1990 period, clouds varied slightly, as shown in Figure 10, and  
349 the observed atmospheric transmission under cloud-free conditions increased (Wild et  
350 al., 2005), which suggests that the large declines in directly observed  $R_s$  and SunDu-  
351 derived  $R_s$  are defective and reinforce the reliability of the adjusted SunDu-derived  $R_s$   
352 (dark red line in Figure 9).

353 From the above analysis, it can be inferred that fewer uncertainties exist in  
354 homogenized SunDu-derived  $R_s$ , which was confirmed by another work that utilized a  
355 different data adjusted method (Stanhill and Cohen, 2008).

### 356 **3.2 Trends of $R_s$ over Japan**

357 The trends of  $R_s$  during specific time periods for different types of datasets are

358 listed in Table 1. Direct measurements of  $R_s$  and SunDu-derived  $R_s$  from 41 selected  
359 stations and all available stations reveal similar variations in  $R_s$  over Japan, which  
360 demonstrates that the sample number has a subtle impact on the estimation of global  
361 brightening and dimming over Japan.

362 A revisit of global dimming and brightening was list in Table 1. Major differences  
363 were found in the time periods of 1961-1980, ranging from -11.2 (-12.0) to -8.4 (-4.8)  
364  $\text{W m}^{-2}$  per decade before and after  $R_s$  homogenizations for all available stations (41  
365 selected stations) over Japan; significant repairs occurred during the 1981-1995 period,  
366 ranging from -10.6 (-11.3) to -1.2 (-1.3)  $\text{W m}^{-2}$  per decade before and after SunDu-  
367 derived  $R_s$  homogenizations for all available stations (41 selected stations) over Japan.  
368 Both corrections were mainly attributed to the homogenization of corrupted raw data  
369 caused by the replacement of instruments for  $R_s$  and SunDu measurements. After  
370 careful checking and adjustment of the SunDu-derived  $R_s$  series, the decadal variation  
371 in  $R_s$  over Japan, which was totally different from former studies (Wild et al., 2005;  
372 Norris and Wild, 2009), was remedied. Direct measurements of  $R_s$  display nearly zero  
373 trend from 1961 to 2014 over Japan, while their homogenization series report a positive  
374 change of 0.8-1.6  $\text{W m}^{-2}$  per decade; SunDu-derived  $R_s$  decrease at a rate of 1.9  $\text{W m}^{-2}$   
375 per decade, while its homogenized series reveals a brightening of 0.9  $\text{W m}^{-2}$  per decade.

376 The combined effects of clouds and aerosols on  $R_s$  make the global dimming and  
377 brightening complicated. The CCRE can explain 70% of global brightening from 1961  
378 to 2014 at monthly and interannual time scales, while the residual radiative effect

379 dominates the decadal variation in  $R_s$ , as shown in Figure 13 and Table 1, which is in  
380 agreement with Wang et al. (2012). Homogenized SunDu-derived  $R_s$  show an increase  
381 of  $1.6 \text{ W m}^{-2}$  per decade from 1961 to 1980; however, persistent increase in cloud  
382 amount yields a CCRE decrease of  $1.1 \text{ W m}^{-2}$  per decade. The residual radiative effect  
383 accounts for an increase of  $2.4 \text{ W m}^{-2}$  per decade for this time period. The cloud  
384 radiative effect ( $-1.4 \text{ W m}^{-2}$  per decade) modulates  $R_s$  variation of  $-1.2 \text{ W m}^{-2}$  per decade  
385 for the 1981-1995 period, while the residual radiative effect ( $1.2 \text{ W m}^{-2}$  per decade)  
386 dominates  $R_s$  variation of  $1.4 \text{ W m}^{-2}$  per decade from 1996 to 2014.

387 Homogenized SunDu-derived  $R_s$  shows a slight increase of  $0.9 \text{ W m}^{-2}$  per decade  
388 from 1961 to 2014 with a 90% confidence interval. However, the CCRE accounts for a  
389 decreased  $R_s$  of  $1.4 \text{ W m}^{-2}$  per decade, which implies that cloud cover changes are not  
390 the primary driving forces for the  $R_s$  trend over Japan. Meanwhile, the residual radiative  
391 effect exhibits an increase of  $2.2 \text{ W m}^{-2}$  per decade, which surpasses the negative CCRE.

392 Several studies demonstrate a generally cleaner sky over Japan from the 1960s to  
393 the 2000s (except for the years impacted by volcanic eruptions) based on atmospheric  
394 transparency and aerosol optical properties (Wild et al., 2005; Kudo et al., 2012), which  
395 supports the dominant role of aerosols in  $R_s$  brightening over Japan, as revealed by the  
396 residual radiative effect here. Furthermore, the residual radiative effect in this study is  
397 stronger than that in Norris and Wild (2009), as raw data were remedied and more  
398 accurate satellite data from CERES were adopted to quantify the radiative effect.  
399 Tsutsumi and Murakami (2012) demonstrate that cloud amount categories exert an

400 important effect on  $R_s$  variation.  $R_s$  enhancement by the increased appearance of large  
401 cloud amounts is superior to  $R_s$  decline by the decreased appearance of small cloud  
402 amounts during 1961-2014, which yields increased  $R_s$  with increasing total cloud  
403 amount. They also pointed out that the decrease in cloud optical thickness due to the  
404 large emissions of  $\text{SO}_2$  and black carbon from East Asia through the aerosol semi-direct  
405 effect (absorption of more energy by aerosols results in the evaporation or suppression  
406 of clouds) may have facilitated the increased  $R_s$  over Japan.

407       The decrease in spring dust storms in March-May during the last 5 decades from  
408 China (Qian et al., 2002; Zhu et al., 2008), which may travel to neighboring  
409 countries(Uno et al., 2008; Choi et al., 2001), could also have triggered the increase in  
410  $R_s$  over Japan. The  $R_s$  variation and radiative effect in different seasons are categorized  
411 in Figure 14 and Table 2, in which an increasing trend of  $1.5 \text{ W m}^{-2}$  per decade in the  
412 homogenized SunDu-derived  $R_s$  prevails in spring for the whole time period, dominated  
413 by a dramatic increase of  $2.8 \text{ W m}^{-2}$  per decade in the residual effect and even larger  
414 increase for 1961-1980 ( $3.1 \text{ W m}^{-2}$  per decade) and 1996-2014 ( $3.4 \text{ W m}^{-2}$  per decade).

#### 415 **4. Data availability**

416       Monthly observed surface incident solar radiation, sunshine duration and cloud  
417 amount data were provided by Japan Meteorological Agency  
418 (<https://www.data.jma.go.jp/obd/stats/data/en/smp/index.html>), and monthly cloud  
419 radiative effect (CRE) data were derived from Clouds and the Earth's Radiant Energy

420 System for CERES EBAF data ([https://ceres.larc.nasa.gov/order\\_data.php](https://ceres.larc.nasa.gov/order_data.php)). The  
421 homogenized observed  $R_s$  and SunDu-derived  $R_s$  used in this study are available at  
422 <https://doi.org/10.11888/Meteoro.tpdc.271524> (Ma et al., 2021).

## 423 **5. Conclusions**

424 The homogenization of raw observations related to  $R_s$  can significantly improve  
425 the accuracy of global dimming and brightening estimation and provide a reliable  
426 assessment of climate trends and variability. In this study, we for the first time  
427 homogenized the raw  $R_s$  observations and obtained a more reliable  $R_s$  data series over  
428 Japan for century-long.

429 Documented artificial shifts in metadata play an important role in regulating the  
430 raw observations. If changepoints were confirmed by metadata or other independent  
431 climate variables, RHtest method was applied to remove the discontinuities. In this  
432 study, shifts in the homogenized raw  $R_s$  were further checked by exploring the  
433 relationship with the ground-based cloud amount and tuned again using homogenized  
434 SunDu-derived  $R_s$  as the reference data. By comparing the variations in independent  
435 climate variables of cloud and aerosol, the homogenized SunDu-derived  $R_s$  were proved  
436 to be more reliable in detecting  $R_s$  variability over Japan.

437 A revisit of global dimming and brightening is made based on the homogenized  
438  $R_s$  series.  $R_s$  over Japan increases at a rate of  $1.6 \text{ W m}^{-2}$  per decade for 1961-1980, which  
439 is contrary to the trend ( $-4.8 \sim -12.0 \text{ W m}^{-2}$  per decade) in the unreasonable  $R_s$

440 observation. A slight decrease of  $1.2 \text{ W m}^{-2}$  per decade for 1981-1995 in homogenized  
441 SunDu-derived  $R_s$  accounts for only 1/10 of the trend in its unadjusted series. This  
442 directly contributes a brightening of  $0.9 \text{ W m}^{-2}$  per decade (with a 99% confidence  
443 interval) for the last 5 decade in homogenized series, which is totally contrary to the  
444 variation in its original series. Global brightening since 1961 over Japan is consistent  
445 with that in Stanhill and Cohen (2008), except that the magnitude is not as large.

446 We also explored how the clouds and aerosols mediate the transformation of  $R_s$ .  
447 The brightening in Japan for 1961-1980 was the combined effect of cloud cover  
448 (negative effect) and aerosols (positive effect). The dimming for 1981-1995 was  
449 governed by reduced cloud amounts, while the increase in  $R_s$  for 1996-2014 was  
450 controlled by decreased aerosols. These results are different from those in Norris and  
451 Wild (2009), as homogenization was performed on the raw data and more accurate  
452 cloud radiative effect data series from CERES were utilized in our study. During the  
453 entire period of 1961-2014, cloud amounts dominated seasonal and interannual  $R_s$   
454 variations, while aerosols (including aerosol-cloud interactions) drove decadal  $R_s$   
455 variations over Japan, noted by other studies, in response to general cleaner skies and a  
456 reduction in spring Asian dust storms (Wang et al., 2012; Kudo et al., 2012).

457

## 458 **Author contributions**

459 QM and KW designed the research and wrote the paper. LS collected the raw data. YH

460 homogenized the raw data. QW provided the technical support. YZ and HL checked the  
461 data.

462

### 463 **Competing interests**

464 The authors declare that they have no conflict of interest.

465



466

467

468

## **Acknowledgements**

469 This study is funded by the National Key R&D Program of China (2017YFA0603601),

470 the National Science Foundation of China (41930970), and Project Supported by State

471 Key Laboratory of Earth Surface Processes and Resource Ecology (2017-KF-03). We

472 thank many institutions for sharing their data: Japan Meteorological Agency for

473 observation data over Japan

474 (<https://www.data.jma.go.jp/obd/stats/data/en/smp/index.html>); Clouds and the Earth's

475 Radiant Energy System for CERES EBAF data

476 ([https://ceres.larc.nasa.gov/order\\_data.php](https://ceres.larc.nasa.gov/order_data.php)). We thank the Expert Team on Climate

477 Change Detection and Indices (ETCCDI) for providing the RHtestV4 homogenization

478 package (<http://etccdi.pacificclimate.org/software.shtml>).

479

480

482 **References**

- 483 Aguilar, E., Auer, I., Brunet, M., Peterson, T. C., and Wieringa, J.: Guidelines on  
484 climate metadata and homogenization, WMO-TD No. 1186, 1186, 2003.
- 485 Alexandersson, H.: A homogeneity test applied to precipitation data, *J. Climatol.*, 6,  
486 661-675, <https://doi.org/10.1002/joc.3370060607>, 1986.
- 487 Allen, R. J., Norris, J. R., and Wild, M.: Evaluation of multidecadal variability in  
488 CMIP5 surface solar radiation and inferred underestimation of aerosol direct effects  
489 over Europe, China, Japan, and India, *J Geophys Res-Atmos*, 118, 6311-6336,  
490 10.1002/jgrd.50426, 2013.
- 491 Augustine, J. A. and Hodges, G. B.: Variability of Surface Radiation Budget  
492 Components Over the U.S. From 1996 to 2019—Has Brightening Ceased?, *J Geophys*  
493 *Res-Atmos*, 126, e2020JD033590, <https://doi.org/10.1029/2020JD033590>, 2021.
- 494 Choi, J. C., Lee, M., Chun, Y., Kim, J., and Oh, S.: Chemical composition and source  
495 signature of spring aerosol in Seoul, Korea, *J Geophys Res-Atmos*, 106, 18067-  
496 18074, <https://doi.org/10.1029/2001JD900090>, 2001.
- 497 Dai, A., Wang, J., Thorne, P. W., Parker, D. E., Haimberger, L., and Wang, X. L.: A  
498 New Approach to Homogenize Daily Radiosonde Humidity Data, *J Climate*, 24, 965-  
499 991, 10.1175/2010jcli3816.1, 2011.
- 500 Du, J., Wang, K., Cui, B., and Jiang, S.: Correction of Inhomogeneities in Observed  
501 Land Surface Temperatures over China, *J Climate*, 33, 8885-8902, 10.1175/jcli-d-19-  
502 0521.1, 2020.
- 503 Dwyer, J. G., Norris, J. R., and Ruckstuhl, C.: Do climate models reproduce observed  
504 solar dimming and brightening over China and Japan?, *J Geophys Res-Atmos*, 115,  
505 <https://doi.org/10.1029/2009JD012945>, 2010.
- 506 Feng, F. and Wang, K.: Merging ground-based sunshine duration observations with  
507 satellite cloud and aerosol retrievals to produce high-resolution long-term surface  
508 solar radiation over China, *Earth Syst. Sci. Data*, 13, 907-922, 10.5194/essd-13-907-  
509 2021, 2021a.
- 510 Feng, F. and Wang, K.: Merging High-Resolution Satellite Surface Radiation Data  
511 with Meteorological Sunshine Duration Observations over China from 1983 to 2017,  
512 *Remote Sens*, 13, 602, <https://doi.org/10.3390/rs13040602>, 2021b.
- 513 He, Y., Wang, K., Zhou, C., and Wild, M.: A Revisit of Global Dimming and  
514 Brightening Based on the Sunshine Duration, *Geophys Res Lett*, 45, 4281-4289,  
515 <https://doi.org/10.1029/2018GL077424>, 2018.
- 516 Inoue, T. and Matsumoto, J.: Seasonal and secular variations of sunshine duration and  
517 natural seasons in Japan, *Int J Climatol*, 23, 1219-1234, 10.1002/joc.933, 2003.
- 518 Kato, S., Loeb, N. G., Rose, F. G., Doelling, D. R., Rutan, D. A., Caldwell, T. E., Yu,  
519 L., and Weller, R. A.: Surface Irradiances Consistent with CERES-Derived Top-of-

520 Atmosphere Shortwave and Longwave Irradiances, *J Climate*, 26, 2719-2740,  
521 10.1175/jcli-d-12-00436.1, 2012.

522 Katsuyama, M.: On comparison between rotating mirror sunshine recorders and  
523 Jordan sunshine recorders, *Weather Service Bulletin*, 54, 169-183, 1987.

524 Kudo, R., Uchiyama, A., Ijima, O., Ohkawara, N., and Ohta, S.: Aerosol impact on the  
525 brightening in Japan, *J Geophys Res-Atmos*, 117,  
526 <https://doi.org/10.1029/2011JD017158>, 2012.

527 Ma, Q., Wang, K. C., and Wild, M.: Impact of geolocations of validation data on the  
528 evaluation of surface incident shortwave radiation from Earth System Models, *J*  
529 *Geophys Res-Atmos*, 120, 6825-6844, 10.1002/2014JD022572, 2015.

530 Ma, Q., He, Y., Wang, K., and Su, L.: Homogenized solar radiation data set over  
531 Japan (1870-2015), National Tibetan Plateau Data Center [dataset],  
532 10.11888/Meteoro.tpdc.271524, 2021.

533 Manara, V., Brunetti, M., Maugeri, M., Sanchez-Lorenzo, A., and Wild, M.: Sunshine  
534 duration and global radiation trends in Italy (1959–2013): To what extent do they  
535 agree?, *J Geophys Res-Atmos*, 122, 4312-4331,  
536 <https://doi.org/10.1002/2016JD026374>, 2017.

537 Manara, V., Brunetti, M., Celozzi, A., Maugeri, M., Sanchez-Lorenzo, A., and Wild,  
538 M.: Detection of dimming/brightening in Italy from homogenized all-sky and clear-  
539 sky surface solar radiation records and underlying causes (1959–2013), *Atmos Chem*  
540 *Phys*, 16, 11145-11161, 10.5194/acp-16-11145-2016, 2016.

541 Manara, V., Beltrano, M. C., Brunetti, M., Maugeri, M., Sanchez-Lorenzo, A.,  
542 Simolo, C., and Sorrenti, S.: Sunshine duration variability and trends in Italy from  
543 homogenized instrumental time series (1936–2013), *J Geophys Res-Atmos*, 120,  
544 3622-3641, <https://doi.org/10.1002/2014JD022560>, 2015.

545 Noguchi, Y.: Solar radiation and sunshine duration in East Asia, *Archives for*  
546 *meteorology, geophysics, and bioclimatology, Series B*, 29, 111-128,  
547 10.1007/BF02278195, 1981.

548 Norris, J. R. and Wild, M.: Trends in aerosol radiative effects over China and Japan  
549 inferred from observed cloud cover, solar “dimming,” and solar “brightening”, *J*  
550 *Geophys Res-Atmos*, 114, <https://doi.org/10.1029/2008JD011378>, 2009.

551 Ohmura, A.: Observed decadal variations in surface solar radiation and their causes, *J*  
552 *Geophys Res-Atmos*, 114, <https://doi.org/10.1029/2008JD011290>, 2009.

553 Qian, W., Quan, L., and Shi, S.: Variations of the Dust Storm in China and its Climatic  
554 Control, *J Climate*, 15, 1216-1229, 10.1175/1520-  
555 0442(2002)015<1216:Votdsi>2.0.Co;2, 2002.

556 Qian, Y., Kaiser, D. P., Leung, L. R., and Xu, M.: More frequent cloud-free sky and  
557 less surface solar radiation in China from 1955 to 2000, *Geophys Res Lett*, 33,  
558 L01812, 10.1029/2005gl024586, 2006.

559 Reeves, J., Chen, J., Wang, X. L., Lund, R., and Lu, Q. Q.: A Review and Comparison  
560 of Change-point Detection Techniques for Climate Data, *J Appl Meteorol Clim*, 46,

561 900-915, 10.1175/jam2493.1, 2007.

562 Robock, A.: Volcanic eruptions and climate, *Rev Geophys*, 38, 191-219,

563 <https://doi.org/10.1029/1998RG000054>, 2000.

564 Sanchez-Lorenzo, A. and Wild, M.: Decadal variations in estimated surface solar

565 radiation over Switzerland since the late 19th century, *Atmos Chem Phys*, 12, 8635-

566 8644, 10.5194/acp-12-8635-2012, 2012.

567 Sanchez-Lorenzo, A., Calbó, J., and Martin-Vide, J.: Spatial and Temporal Trends in

568 Sunshine Duration over Western Europe (1938–2004), *J Climate*, 21, 6089-6098,

569 10.1175/2008jcli2442.1, 2008.

570 Sanchez-Lorenzo, A., Calbó, J., and Wild, M.: Global and diffuse solar radiation in

571 Spain: Building a homogeneous dataset and assessing their trends, *Global Planet*

572 *Change*, 100, 343-352, <https://doi.org/10.1016/j.gloplacha.2012.11.010>, 2013.

573 Sanchez-Lorenzo, A., Brunetti, M., Calbó, J., and Martin-Vide, J.: Recent spatial and

574 temporal variability and trends of sunshine duration over the Iberian Peninsula from a

575 homogenized data set, *J Geophys Res-Atmos*, 112,

576 <https://doi.org/10.1029/2007JD008677>, 2007.

577 Sanchez-Lorenzo, A., Wild, M., Brunetti, M., Guijarro, J. A., Hakuba, M. Z., Calbó,

578 J., Mystakidis, S., and Bartok, B.: Reassessment and update of long-term trends in

579 downward surface shortwave radiation over Europe (1939–2012), *J Geophys Res-*

580 *Atmos*, 120, 9555-9569, <https://doi.org/10.1002/2015JD023321>, 2015.

581 Sato, M., Hansen, J. E., McCormick, M. P., and Pollack, J. B.: Stratospheric aerosol

582 optical depths, 1850–1990, *J Geophys Res-Atmos*, 98, 22987-22994,

583 <https://doi.org/10.1029/93JD02553>, 1993.

584 Shi, G. Y., Hayasaka, T., Ohmura, A., Chen, Z. H., Wang, B., Zhao, J. Q., Che, H. Z.,

585 and Xu, L.: Data quality assessment and the long-term trend of ground solar radiation

586 in China, *J Appl Meteorol Clim*, 47, 1006-1016, 10.1175/2007jamc1493.1, 2008.

587 Stanhill, G. and Cohen, S.: Solar Radiation Changes in the United States during the

588 Twentieth Century: Evidence from Sunshine Duration Measurements, *J Climate*, 18,

589 1503-1512, 10.1175/jcli3354.1, 2005.

590 Stanhill, G. and Cohen, S.: Solar Radiation Changes in Japan during the 20th Century:

591 Evidence from Sunshine Duration Measurements, *J Meteorol Soc Jpn. Ser. II*, 86, 57-

592 67, 10.2151/jmsj.86.57, 2008.

593 Tanaka, K., Ohmura, A., Folini, D., Wild, M., and Ohkawara, N.: Is global dimming

594 and brightening in Japan limited to urban areas?, *Atmospheric Chemistry And*

595 *Physics*, 16, 13969-14001, 10.5194/acp-16-13969-2016, 2016.

596 Tang, W. J., Yang, K., Qin, J., Cheng, C. C. K., and He, J.: Solar radiation trend across

597 China in recent decades: a revisit with quality-controlled data, *Atmos Chem Phys*, 11,

598 393-406, 10.5194/acp-11-393-2011, 2011.

599 Tsutsumi, Y. and Murakami, S.: Increase in Global Solar Radiation with Total Cloud

600 Amount from 33 Years Observations in Japan, *J Meteorol Soc Jpn*, 90, 575-581,

601 10.2151/jmsj.2012-409, 2012.

602 Uno, I., Yumimoto, K., Shimizu, A., Hara, Y., Sugimoto, N., Wang, Z., Liu, Z., and  
603 Winker, D. M.: 3D structure of Asian dust transport revealed by CALIPSO lidar and a  
604 4DVAR dust model, *Geophys Res Lett*, 35, <https://doi.org/10.1029/2007GL032329>,  
605 2008.

606 Vincent, L. A., Wang, X. L., Milewska, E. J., Wan, H., Yang, F., and Swail, V.: A  
607 second generation of homogenized Canadian monthly surface air temperature for  
608 climate trend analysis, *J Geophys Res-Atmos*, 117,  
609 <https://doi.org/10.1029/2012JD017859>, 2012.

610 Wang, K. C., Dickinson, R. E., Wild, M., and Liang, S.: Atmospheric impacts on  
611 climatic variability of surface incident solar radiation, *Atmos Chem Phys*, 12, 9581-  
612 9592, 10.5194/acp-12-9581-2012, 2012.

613 Wang, K. C., Ma, Q., Li, Z. J., and Wang, J. K.: Decadal variability of surface incident  
614 solar radiation over China: Observations, satellite retrievals, and reanalyses, *J*  
615 *Geophys Res-Atmos*, 120, 6500-6514, 10.1002/2015JD023420, 2015.

616 Wang, K. C., Dickinson, R. E., Ma, Q., Augustine, J. A., and Wild, M.: Measurement  
617 Methods Affect the Observed Global Dimming and Brightening, *J Climate*, 26, 4112-  
618 4120, 10.1175/Jcli-D-12-00482.1, 2013.

619 Wang, X. L.: Comments on “Detection of Undocumented Change-points: A Revision  
620 of the Two-Phase Regression Model”, *J Climate*, 16, 3383-3385, 10.1175/1520-  
621 0442(2003)016<3383:Codouc>2.0.Co;2, 2003.

622 Wang, X. L.: Accounting for Autocorrelation in Detecting Mean Shifts in Climate  
623 Data Series Using the Penalized Maximal t or F Test, *J Appl Meteorol Clim*, 47, 2423-  
624 2444, 10.1175/2008jamc1741.1, 2008a.

625 Wang, X. L., Wen, Q. H., and Wu, Y.: Penalized Maximal t Test for Detecting  
626 Undocumented Mean Change in Climate Data Series, *J Appl Meteorol Clim*, 46, 916-  
627 931, 10.1175/jam2504.1, 2007.

628 Wang, X. L. L.: Penalized maximal F test for detecting undocumented mean shift  
629 without trend change, *J Atmos Ocean Technol*, 25, 368-384,  
630 10.1175/2007JTECHA982.1, 2008b.

631 Wang, X. L. L., Chen, H. F., Wu, Y. H., Feng, Y., and Pu, Q. A.: New Techniques for  
632 the Detection and Adjustment of Shifts in Daily Precipitation Data Series, *J Appl*  
633 *Meteorol Clim*, 49, 2416-2436, 10.1175/2010JAMC2376.1, 2010.

634 Wild, M. and Schmucki, E.: Assessment of global dimming and brightening in IPCC-  
635 AR4/CMIP3 models and ERA40, *Clim Dynam*, 37, 1671-1688, 10.1007/s00382-010-  
636 0939-3, 2011.

637 Wild, M., Wacker, S., Yang, S., and Sanchez-Lorenzo, A.: Evidence for Clear-Sky  
638 Dimming and Brightening in Central Europe, *Geophys Res Lett*, 48, e2020GL092216,  
639 <https://doi.org/10.1029/2020GL092216>, 2021.

640 Wild, M., Gilgen, H., Roesch, A., Ohmura, A., Long, C. N., Dutton, E. G., Forgan, B.,  
641 Kallis, A., Russak, V., and Tsvetkov, A.: From Dimming to Brightening: Decadal  
642 Changes in Solar Radiation at Earth's Surface, *Science*, 308, 847-850,

643 10.1126/science.1103215, 2005.  
644 Witham, C. S.: Volcanic disasters and incidents: A new database, *J Volcanol Geoth*  
645 *Res*, 148, 191-233, 10.1016/j.jvolgeores.2005.04.017, 2005.  
646 Xia, X.: A closer looking at dimming and brightening in China during 1961-2005,  
647 *Ann Geophys*, 28, 1121-1132, 10.5194/angeo-28-1121-2010, 2010.  
648 Yang, K., Koike, T., and Ye, B. S.: Improving estimation of hourly, daily, and monthly  
649 solar radiation by importing global data sets, *Agr Forest Meteorol*, 137, 43-55,  
650 10.1016/j.agrformet.2006.02.001, 2006.  
651 Yang, S., Wang, X. L., and Wild, M.: Homogenization and Trend Analysis of the  
652 1958–2016 In Situ Surface Solar Radiation Records in China, *J Clim*, 31, 4529-4541,  
653 10.1175/jcli-d-17-0891.1, 2018.  
654 Zeng, Z., Wang, Z., Gui, K., Yan, X., Gao, M., Luo, M., Geng, H., Liao, T., Li, X.,  
655 An, J., Liu, H., He, C., Ning, G., and Yang, Y.: Daily Global Solar Radiation in China  
656 Estimated From High-Density Meteorological Observations: A Random Forest Model  
657 Framework, *Earth Space Sci.*, 7, e2019EA001058,  
658 <https://doi.org/10.1029/2019EA001058>, 2020.  
659 Zhou, C., Wang, J., Dai, A., and Thorne, P. W.: A New Approach to Homogenize  
660 Global Subdaily Radiosonde Temperature Data from 1958 to 2018, *J Climate*, 34,  
661 1163-1183, 10.1175/jcli-d-20-0352.1, 2021.  
662 Zhu, C., Wang, B., and Qian, W.: Why do dust storms decrease in northern China  
663 concurrently with the recent global warming?, *Geophys Res Lett*, 35,  
664 <https://doi.org/10.1029/2008GL034886>, 2008.  
665  
666

667 Table 1. Trends of Surface Incident Solar Radiation ( $R_s$ ) in Japan during Specific Time  
668 Periods for Different Types of Datasets<sup>a</sup>. Unit: W m<sup>-2</sup> per decade  
669

| Case <sup>b</sup>          | Datasets <sup>c</sup> | 1961-1980 | 1981-1995 | 1996-2014 | 1961-2014 |
|----------------------------|-----------------------|-----------|-----------|-----------|-----------|
| Selected<br>41<br>Stations | OBS-raw               | -12.0**   | -2.1      | 2.4       | -0.3      |
|                            | OBS_HM                | -4.8*     | -2.1      | 2.4       | 1.5**     |
|                            | OBS_2HM               | -0.8*     | -2.1      | 2.4*      | 0.9**     |
|                            | SunDu-derived         | 1.4       | -11.3**   | 1.4       | -2.1**    |
|                            | SunDu-derived_HM      | 1.4       | -1.3*     | 1.5       | 0.9**     |
| All<br>Stations            | OBS-raw               | -11.2**   | -1.3      | 2.2       | 0.2       |
|                            | OBS_HM                | -8.4**    | -1.3      | 2.2       | 0.8       |
|                            | OBS_2HM               | 0.7       | -1.3      | 2.2       | 1.6**     |
|                            | SunDu-derived         | 2.3*      | -10.6**   | 1.2       | -1.9**    |
|                            | SunDu-derived_HM      | 1.6       | -1.2      | 1.4       | 0.9*      |
| Radiative<br>Effect        | CCRE series           | -1.1      | -1.4      | -0.0      | -1.4**    |
|                            | Residual series       | 2.4**     | -0.1      | 1.2*      | 2.2**     |

670

671

672

673 <sup>a</sup>The trend calculations were based on the linear regression method. Values with two  
674 asterisks (\*\*) imply  $p < 0.01$ , and those with one asterisk (\*) imply  $0.01 < p < 0.1$ .

675 <sup>b</sup> $R_s$  trends were calculated by different numbers of observations, including all stations  
676 that are available on the JMA website and 41 stations (marked with red in Table S1,  
677 detailed in Section 3.1) that are significantly improved after homogenization. This  
678 implies that the sample number has a subtle impact on the trend calculation over Japan.  
679 Radiative effects from clouds and aerosols were also explored.

680 <sup>c</sup>Trend calculations were based on the raw measurements of surface incident solar  
681 radiation (OBS-raw), their homogenized series (OBS\_HM), derived incident solar  
682 radiation from sunshine duration hours (SunDu-derived) and their homogenized series  
683 (SunDu-derived\_HM). OBS\_HM from 1961 to 1970 was further homogenized by  
684 using SunDu-derived\_HM as reference data, termed OBS\_2HM. It is found that

685 homogenized SunDu-derived  $R_s$  have the lowest uncertainties among these five  
686 datasets in Section 3.1. The cloud cover radiative effect (CCRE) was denoted as the  
687 change in  $R_s$  produced by a change in cloud cover, and the CCRE calculations were  
688 performed following Equation (4) by observed cloud amounts and the cloud radiative  
689 effect (CRE) from CERES satellite retrieval. Residual effect series were obtained by  
690 removing the CCRE from homogenized SunDu-derived  $R_s$  anomalies.  
691

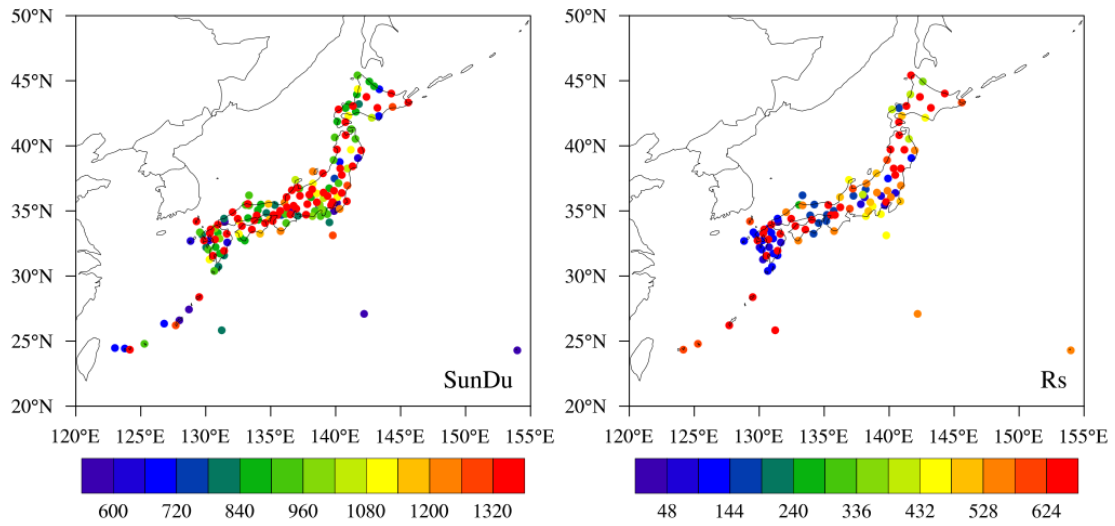


692

693 Table 2. Trends of Surface Incident Solar Radiation ( $R_s$ ) in Japan during Specific Time694 Periods for Different Types of Datasets for All Seasons. Unit:  $W m^{-2}$  per decade

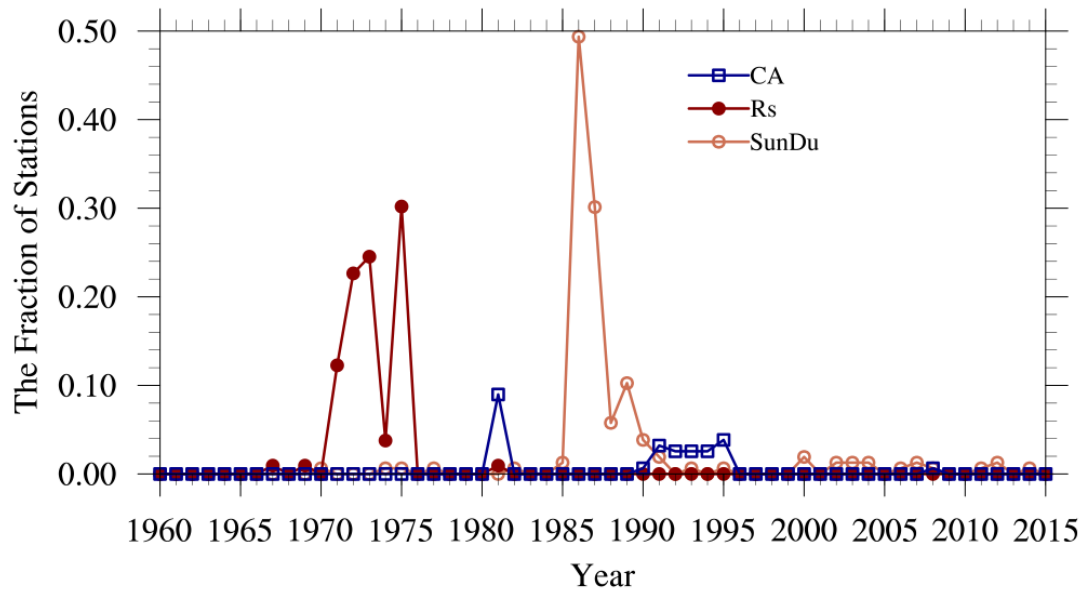
| Season | Datasets         | 1961-1980 | 1981-1995 | 1996-2014 | 1961-2014 |
|--------|------------------|-----------|-----------|-----------|-----------|
| Spring | SunDu-derived_HM | 3.1       | -1.5      | 3.4*      | 1.5       |
|        | CCRE series      | -0.7      | -1.6      | -1.6      | -0.9      |
|        | Residual series  | 4.9**     | -0.5**    | 2.2**     | 2.8*      |
| Summer | SunDu-derived_HM | 1.4       | -3.4      | 0.6       | 0.4       |
|        | CCRE series      | -1.9      | -2.1      | -4.4**    | -2.7      |
|        | Residual series  | 2.0**     | -1.8      | 1.5**     | 2.8       |
| Autumn | SunDu-derived_HM | 0.6       | 1.5       | 3.3**     | 1.0*      |
|        | CCRE series      | -1.3**    | 1.6       | 1.6       | -0.9      |
|        | Residual series  | 1.8**     | 0.8**     | 2.1**     | 2.0*      |
| Winter | SunDu-derived_HM | 0.6       | -1.5      | -1.6      | 0.5       |
|        | CCRE series      | -0.6      | -3.3      | -0.6      | -0.7      |
|        | Residual series  | 1.1**     | 0.9**     | -0.9**    | 1.2**     |

695



696

697 Figure 1. The spatial distribution of stations over Japan with observed sunshine duration  
 698 (SunDu, 156 stations) and surface incident solar radiation ( $R_s$ , 105 stations) data. The  
 699 colours indicate the data length of the SunDu records from 1890 to 2015 and  $R_s$  records  
 700 from 1961 to 2015. Unit: month.



701

702 Figure 2. The fraction of stations that suffer from data inhomogeneity due to site

703 relocation, change of instruments and measurement method for sunshine duration

704 (SunDu) records, cloud amount (CA) records and surface incident solar radiation ( $R_s$ )

705 records. In total, there were 156 stations with SunDu records, 105 of which had  $R_s$

706 records and 155 of which had CA records. The inhomogeneity information shown here

707 was derived from metadata from

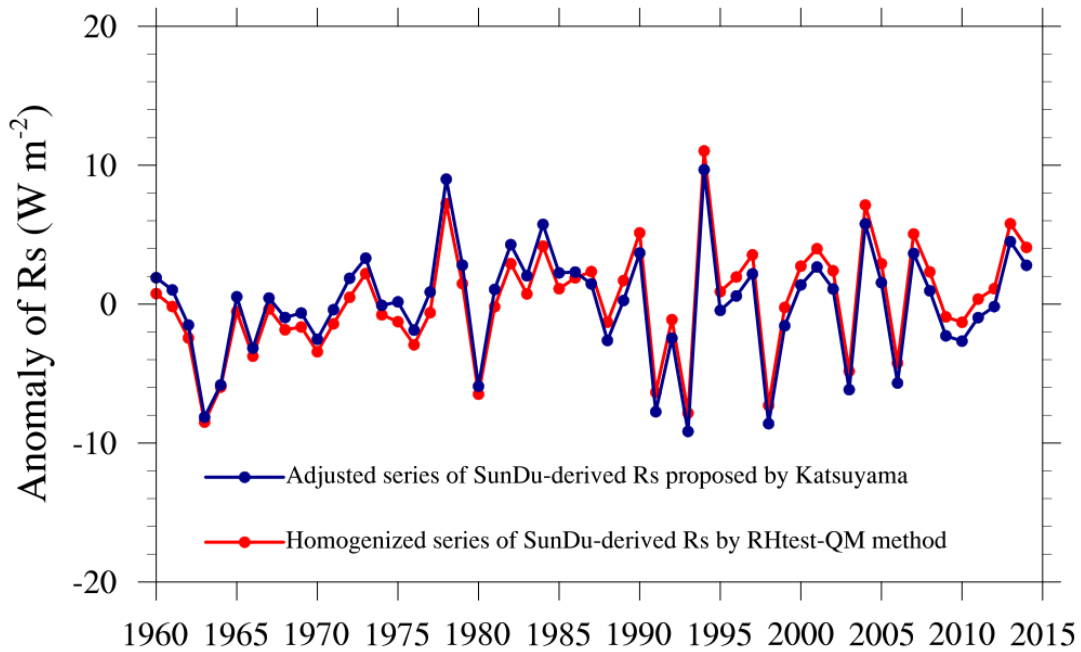
708 <https://www.data.jma.go.jp/obd/stats/data/en/smp/index.html>, and was used as primary

709 information to perform the inhomogeneity adjustment in the RHtest method detailed in

710 Section 2.2.

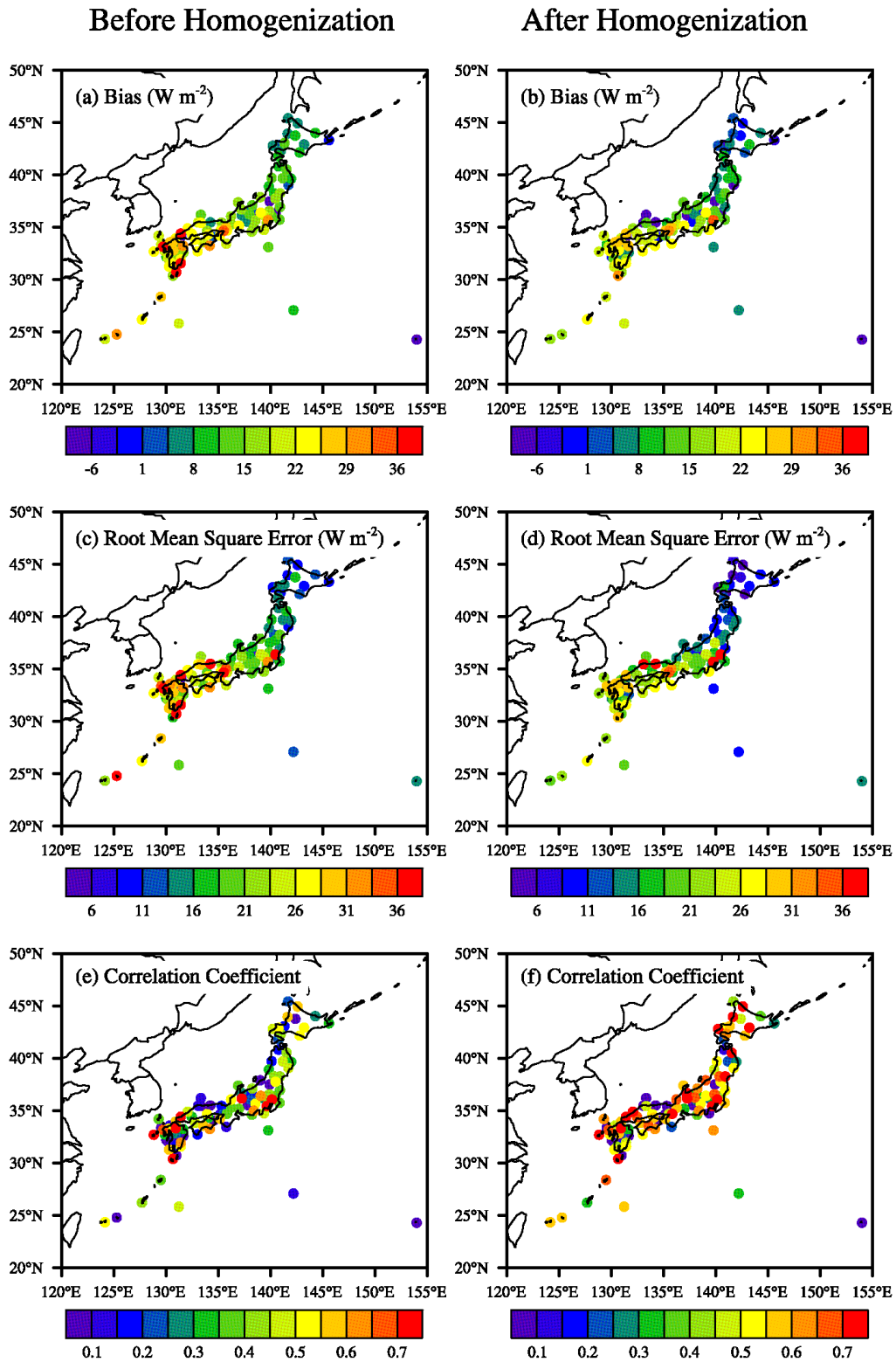
711

712



713

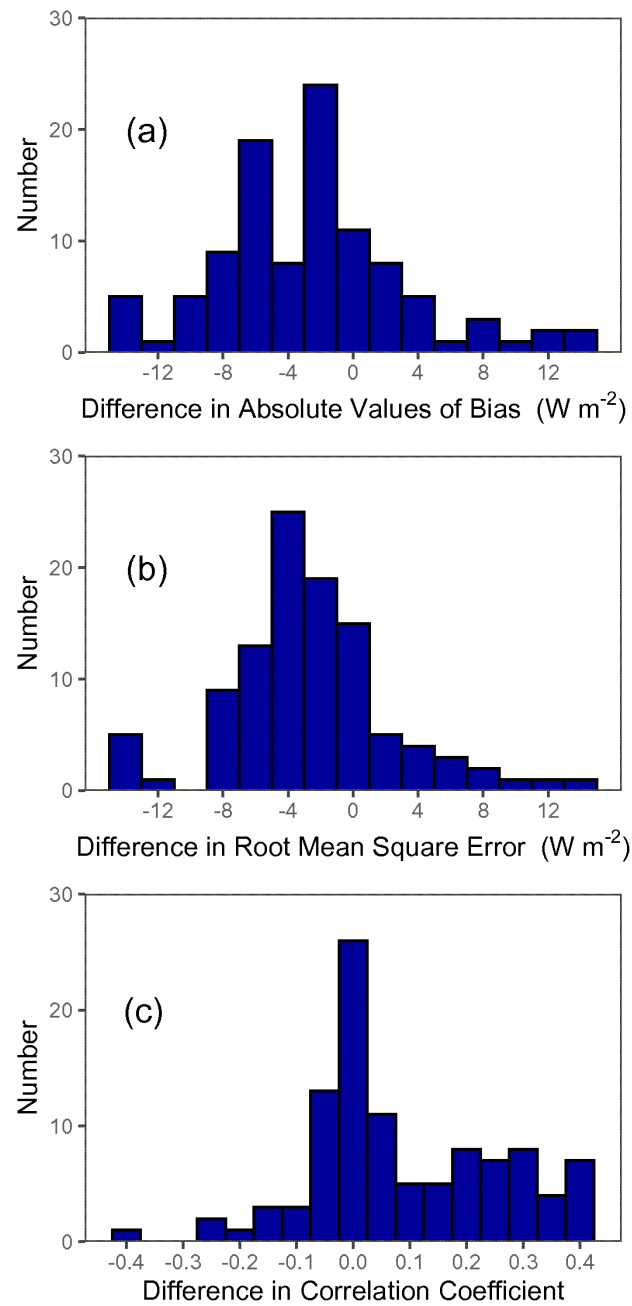
714 Figure 3. The anomalies of surface incident solar radiation ( $R_s$ ) derived from  
 715 homogenized sunshine duration (SunDu) data (red line) by the RHtest-QM method  
 716 and other independent data (blue line) adjusted by the method in (Katsuyama, 1987).  
 717 Both of the homogenized datasets yield nearly the same  $R_s$  variation.



718

719 Figure 4. The spatial distribution of bias, root mean square error and correlation  
 720 coefficient between SunDu-derived surface incident solar radiation ( $R_s$ ) and observed

721  $R_s$  before (a, c, e) and after (b, d, f) homogenization. Improvements were made at  
722 most sites after homogenization.  
723



725

726 Figure 5. Histograms of the difference in absolute values of bias, root mean square

727 error and correlation coefficient between SunDu-derived surface incident solar

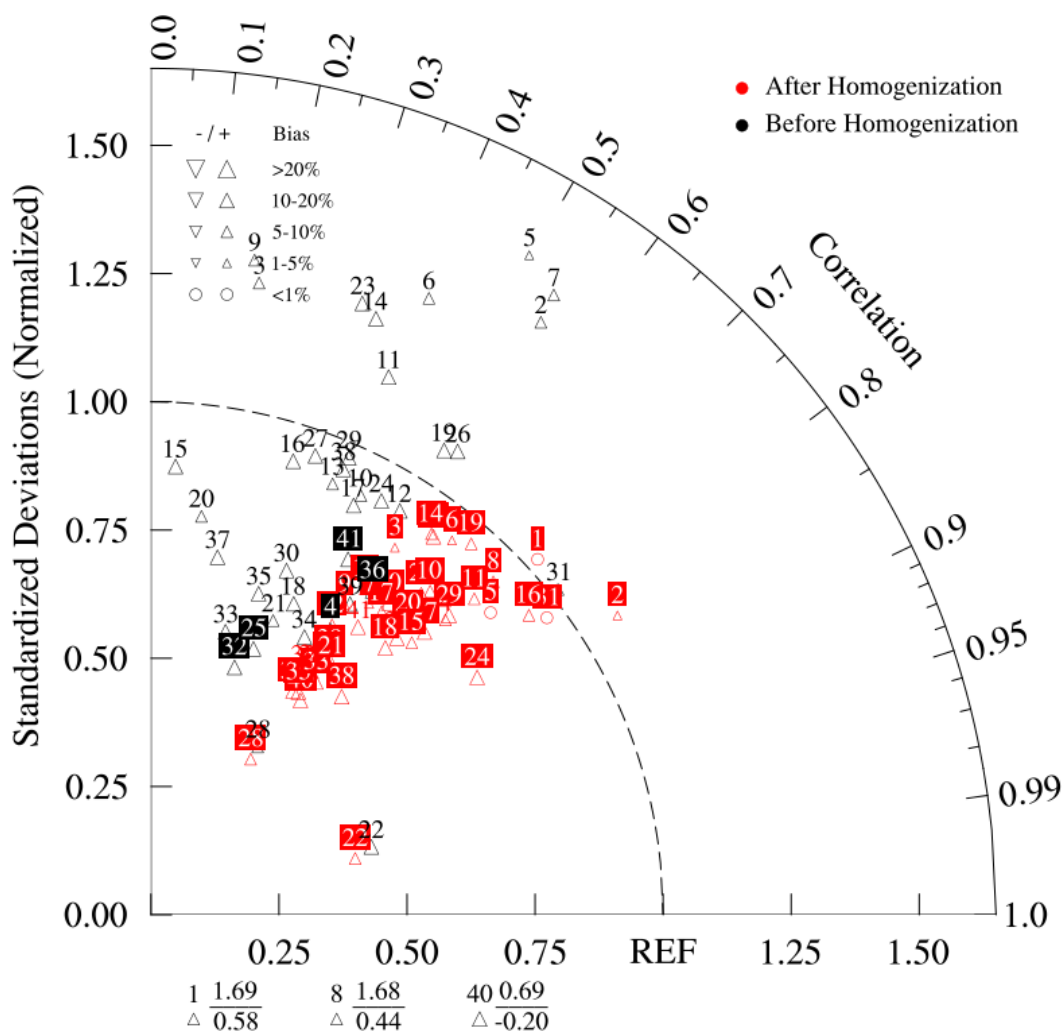
728 radiation ( $R_s$ ) and observed  $R_s$  before and after homogenization. Their differences

729 decrease after homogenization.

730

731

732



733

734

735 Figure 6. Taylor diagram describing the relative biases, standardized deviations and

736 correlation coefficients between the annual observed surface incident shortwave

737 radiation (Rs) and annual sunshine duration (SunDu) derived Rs before and after

738 homogenization at 41 selected stations (Numbered 1-41 here). “REF” can be treated as

739 the perfect point, where values the closer to this point indicate a better evaluation. The

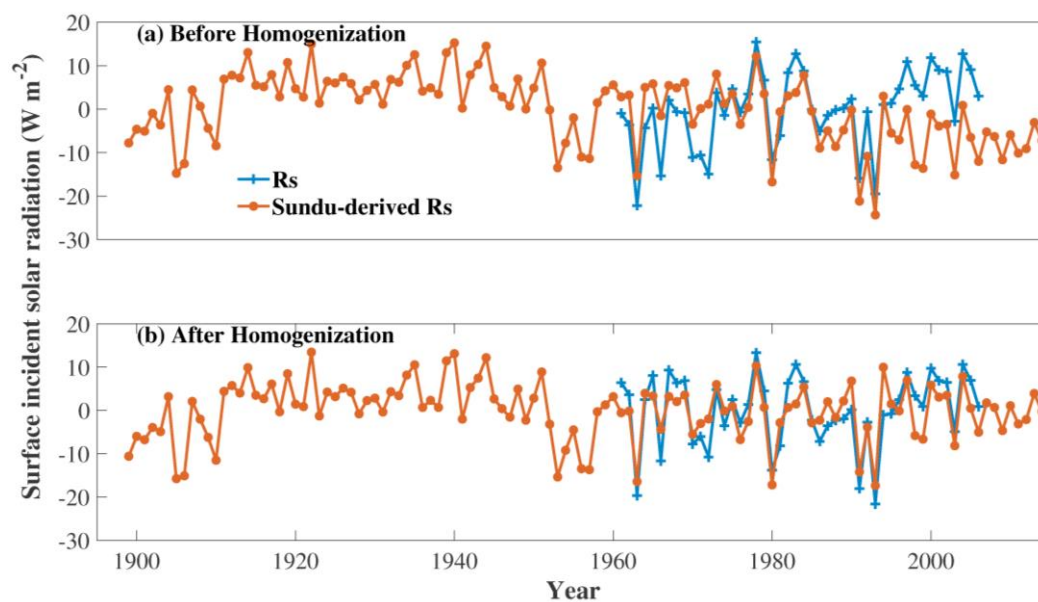


740 size and direction of the triangles denote the magnitude and negative or positive of  
741 biases, respectively. The boxes indicate the smaller bias in Raw (black color) or HM  
742 (red color) series. This figure shows that biases decrease at most sites (in red boxes)  
743 after homogenization, except for the 5 stations numbered 4, 25, 32, 36 and 41 (in black  
744 boxes). Three stations (numbered 1, 8 and 40 in black color) listed below the panel are  
745 beyond the scope of the figure, with bias (triangle), ratio of standardized deviation  
746 (above the “---” line) and correlation coefficient (below the “---” line) shown. In  
747 addition to the improvements in the correlation coefficients after homogenization, the  
748 biases and the standard deviations generally become small in this Taylor diagram.

749

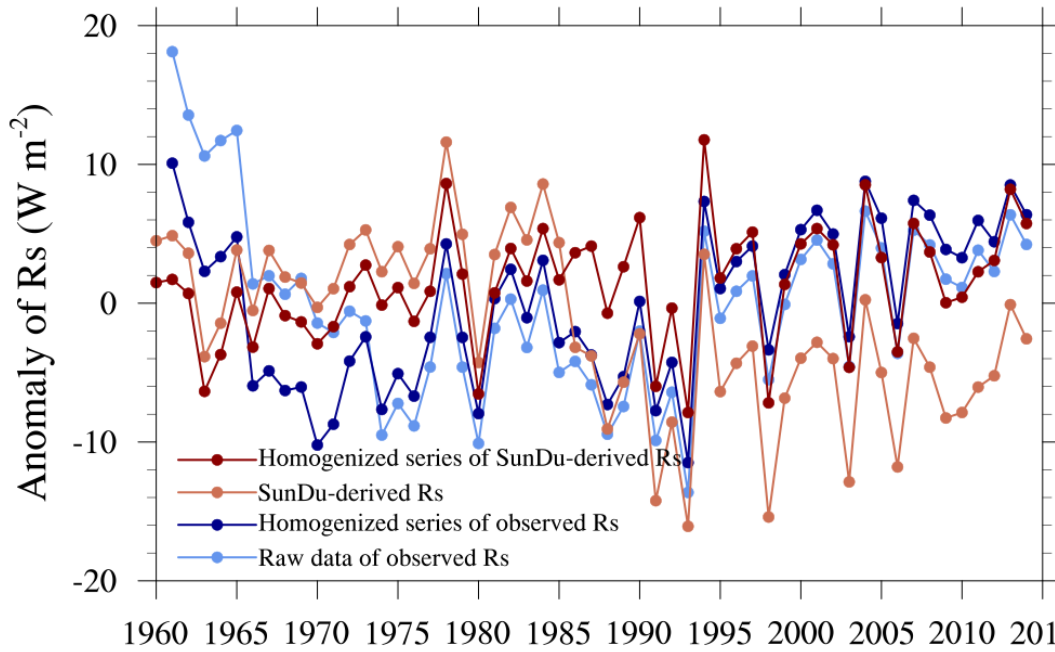
750

751  
752  
753



754  
755  
756  
757  
758  
759  
760

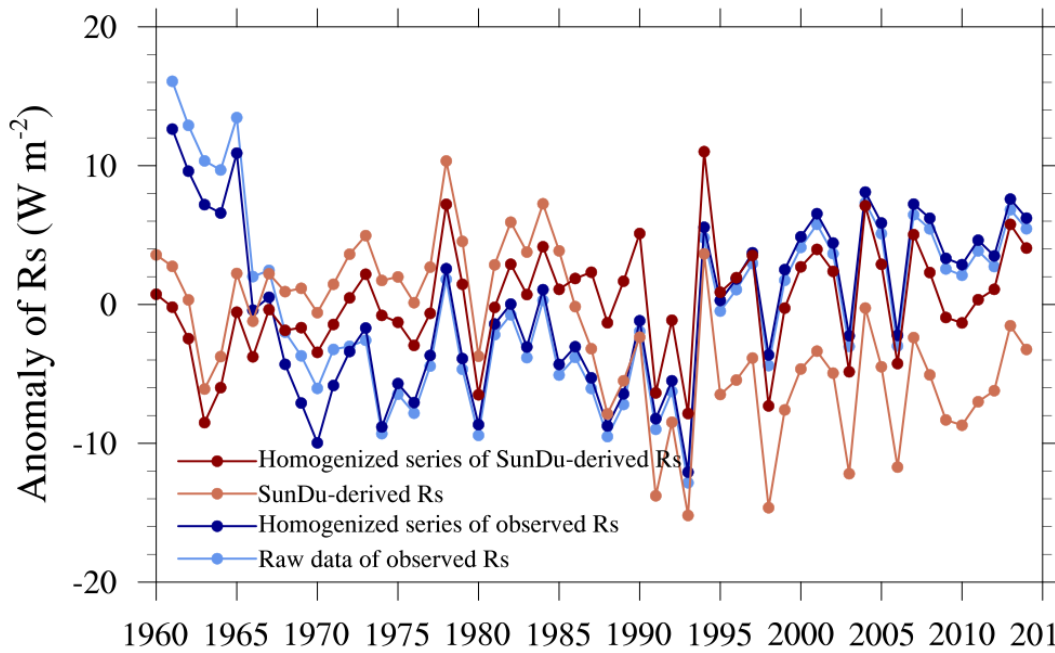
Figure 7. Time series of annual anomalies of observed surface incident solar radiation ( $R_s$ ) and SunDu-derived  $R_s$  at HAMADA site (WMO-ID: 47755, Lat:  $34.9^\circ$ , Lon: 132.07) before and after homogenization.



761

762 Figure 8. Time series of annual anomalies of surface incident solar radiation ( $R_s$ ) based  
 763 on direct  $R_s$  observations (light blue line) and their homogenized series (dark blue line)  
 764 and sunshine duration (SunDu) derived  $R_s$  (light red line) and their homogenized series  
 765 (dark red line). All of the lines were calculated based on observations at 41 sites. Details  
 766 on how these 41 sites were selected are given in Section 3.1. The  $R_s$  variations are nearly  
 767 the same as those shown in Figure 7, which were calculated based on all available  
 768 observations.

769

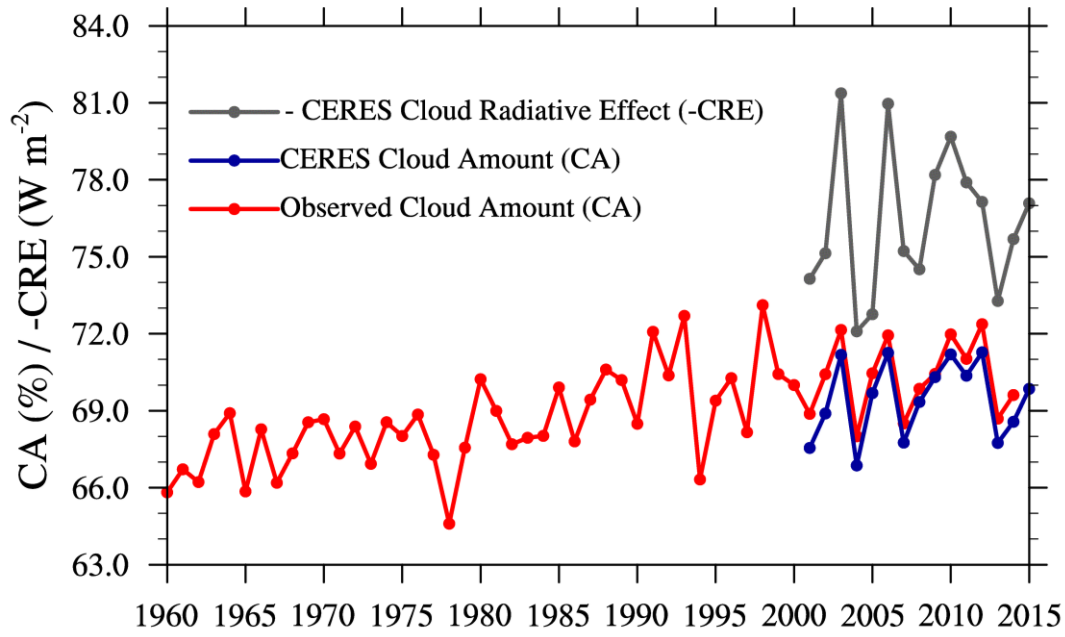


770

771 Figure 9. Time series of annual anomalies of the surface incident solar radiation ( $R_s$ )  
 772 based on direct observations (light blue line) and their homogenized series (dark blue  
 773 line) and sunshine duration (SunDu) derived  $R_s$  (light red line) and their homogenized  
 774 series (dark red line). All of the lines were calculated based on as many observations as  
 775 possible. The light blue line and dark blue line were calculated from the  $R_s$  observations  
 776 at 105 sites, while the light red line and dark red line were derived from the SunDu-  
 777 derived  $R_s$  at 156 sites. The  $R_s$  variations are nearly the same as those shown in Figure  
 778 6, which were calculated based on the 41 selected sites in Section 3.1. Large  
 779 discrepancies were found in the homogenized data series (dark blue and dark red lines).

780

781



782

783 Figure 10. The cloud amount (CA) from CERES (blue line) agrees well with that  
 784 derived from surface observations (red line) over Japan. At the annual time scale, the  
 785 negative cloud radiative effect (-CRE, grey line) in CERES correlated well with the  
 786 cloud amount.

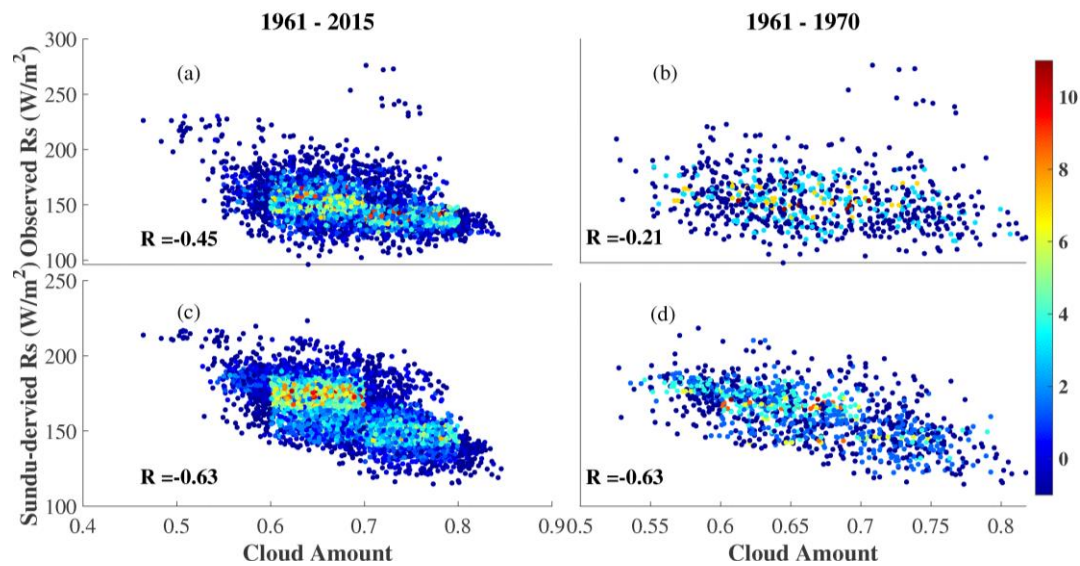
787

788

789

790

791



792

793 Figure 11. Scatter plot of homogenized monthly surface incident solar radiation ( $R_s$ )

794 (observed and SunDu-derived solar radiation) as a function of ground-based

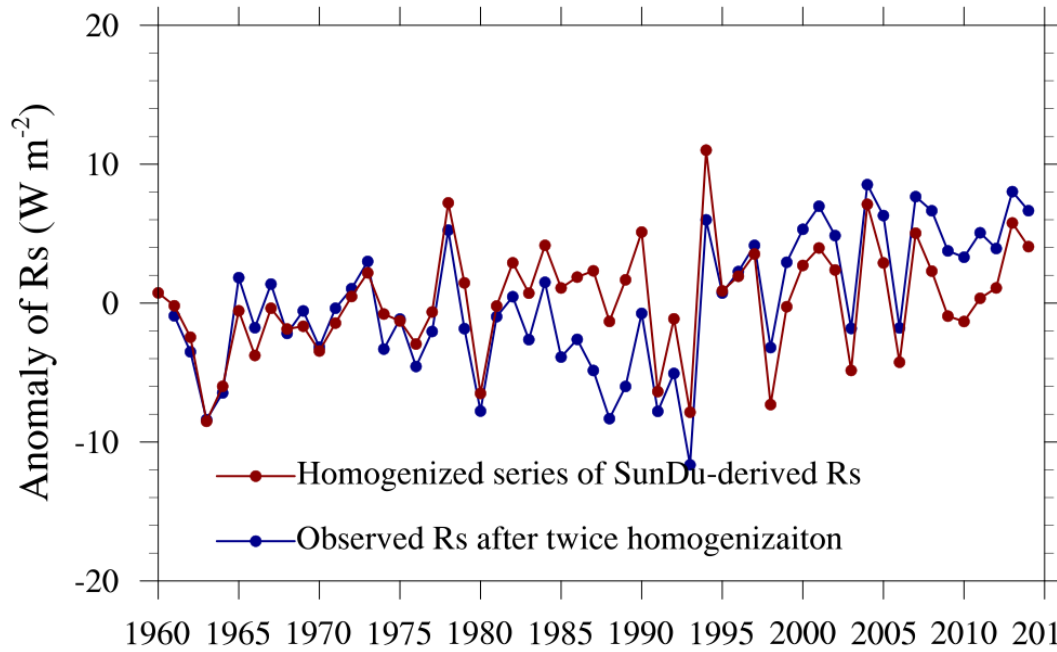
795 observations of cloud amount over Japan at all stations only when both cloud amount

796 data and observed  $R_s$  data are available. (a) and (c) for 1961-2015, (b) and (d) for

797 1961-1970. The smallest correlation coefficient in (b) indicates that the observed  $R_s$

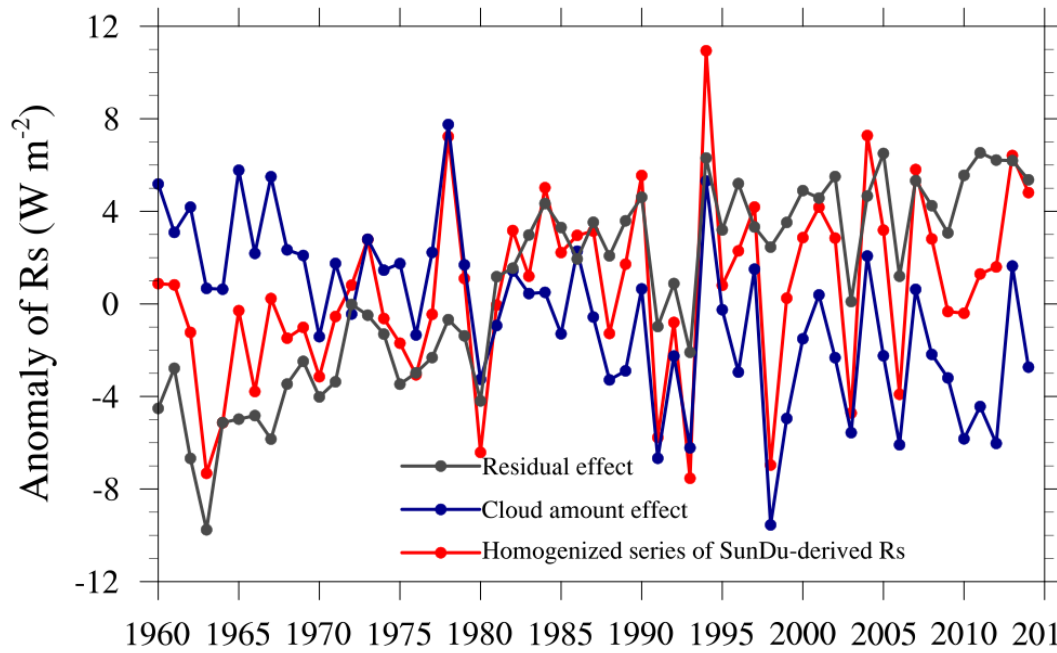
798 data are spurious for 1961-1970, and SunDu-derived  $R_s$  are more convincing.

799



800

801 Figure 12. Time series of annual anomalies of the surface incident solar radiation ( $R_s$ )  
 802 based on  $R_s$  observations after two homogenizations (dark blue line). The homogenized  
 803 series of observed  $R_s$  from 1961 to 1970 shown in Figure 7 was tuned by RHtest method  
 804 again using the homogenized series of SunDu-derived  $R_s$  (dark red line in Figure 7 and  
 805 Figure 10) as a reference.

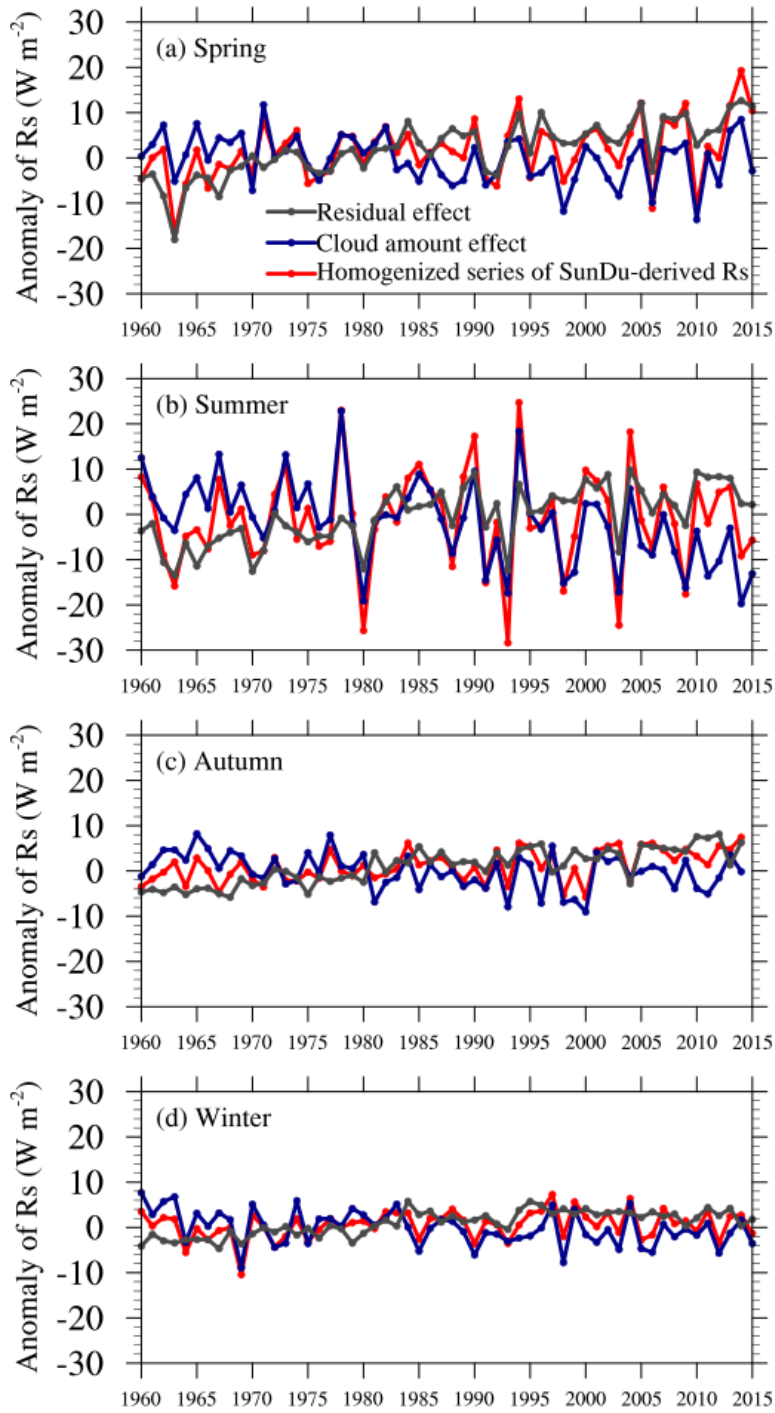


806

807 Figure 13. Area-averaged anomalies of homogenized SunDu-derived  $R_s$  (red line) over  
 808 Japan. The cloud cover radiative effect (CCRE, blue line) was denoted as the change in  
 809  $R_s$  produced by a change in cloud cover and calculated following Equation (4) by  
 810 observed cloud amounts and cloud radiative effect (CRE) from the CERES satellite  
 811 retrieval. The residual effect (grey line) was obtained by removing the cloud cover  
 812 radiative effect (CCRE) from the homogenized SunDu-derived  $R_s$  anomalies.

813





814

815 Figure 14. Same as Figure 12 but for the four seasons. The decrease in Asian spring

816 dust may have triggered the brightening over Japan for 1961-2015, as the  $R_s$  in spring

817 increases most among the seasons.